A novel, wave-shaped profile of germline selection of pathogenic mtDNA mutations is discovered by bypassing a classical statistical bias.

Auden Cote-L'Heureux[1]*, Zoë Fleischmann[1]*, Melissa Franco[1]*, Zhibin Chen[1]*, Mark Khrapko[1], Benjamin Vyshedskiy[2], Maxim Braverman[3], Konstantin Popadin [4,5,6], Sarah Pickett[7], Dori C. Woods[1], Jonathan L. Tilly[1], Douglas Turnbull[7], Konstantin Khrapko[1]**.

[1]Department of Biology Northeastern University, Boston, Massachusetts, USA
[2]Cambridge University, Cambridge, UK
[3]Department of Mathematics, Northeastern University, Boston, Massachusetts, USA
[4]School of Life Sciences, École Polytechnique Fédérale de Lausanne, and [5]Swiss Institute of Bioinformatics, Lausanne, Switzerland
[6]Center for Mitochondrial Functional Genomics, IImmanuel Kant Baltic Federal University, Kaliningrad, Russia.
[7]Wellcome Centre for Mitochondrial Research, Translational and Clinical Research Institute, Newcastle University, Newcastle upon Tyne, UK *Equal contribution ** correspondence: k.khrapko@northeastern.com

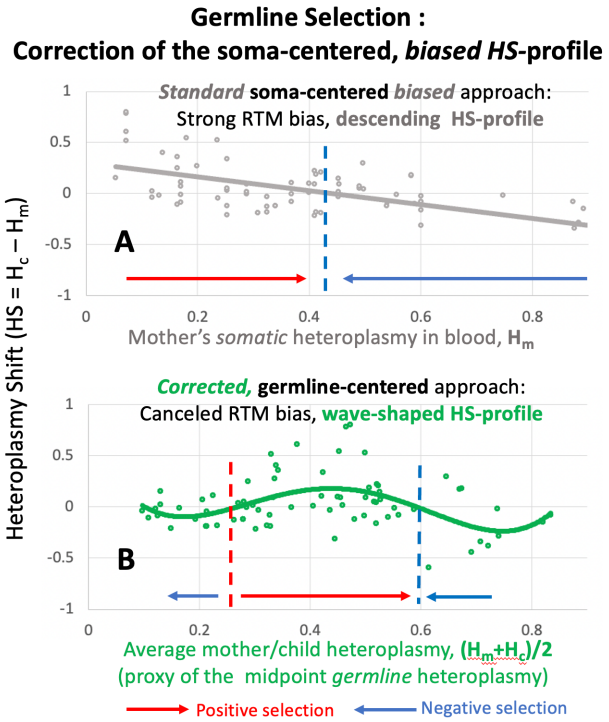

Figure 1 (Graphic Summary) Pathogenic mtDNA mutations that cause a host of devastating inherited diseases are usually thought to follow a surprising inheritance trend: Mothers with low levels of mutation (heteroplasmy, H_m) tend to bear children with higher heteroplasmy then their own (positive Heteroplasmy Shift, HS). In contrast, mothers with high heteroplasmy bear children with decreased heteroplasmy (negative HS).

In **Fig. 1A** this trend is illustrated for the most prevalent pathogenic mtDNA mutation, 3243A>G, causing MELAS (Mitochondrial encephalomyopathy, lactic acidosis and stroke-like episodes). Each dot represents a heteroplasmy shift in a mother/child pair, plotted as a function of mother's heteroplasmy (H_m). The bold descending "HS profile" (grey regression line) is commonly (and intuitively) explained by the force of the corresponding 'germline selection profile'. i.e., positive selection at low H_m, gradually decreasing and turning negative at high H_m (**Suppl. Note 1**). We demonstrate, however, that this intuitive interpretation is totally incorrect: in fact, the decrease of HS is mostly driven by the classical statistical bias, the RTM (Regression To the Mean). RTM, in turn, results from random variance in the data generated presumably by germline and somatic mtDNA bottlenecks and measurement error. We further show that RTM can be nullified by using the average mother/child heteroplasmy, $(H_m+H_{ch})/2$ as the independent variable, instead of the conventional H_m. Additionally, $(H_m+H_{ch})/2$ is a better proxy of the *germline* heteroplasmy than either H_m or H_{ch}, which are measured in the *soma* (blood).

In **Fig. 1B**, the combined effect of the removal of the RTM bias and of the use of the germline heteroplasmy proxy $(H_m+H_{ch})/2$, results in the rectification of the biased descending HS/selection profile into an unbiased wave-shaped profile (green fourth-order regression curve). We then used simulations to confirm that a combination of RTM bias and wave-shaped selection indeed led to the observed mother-child inheritance patterns, down to the fine detail. We further demonstrated that other pathogenic mtDNA mutations when corrected for the RTM bias by the use of the $(H_m+H_{ch})/2$ variable mostly also exhibit wave-shaped germline selection patterns. *Note*: selection does not necessarily converge to zero at high and low heteroplasmy as it may look in **Fig. 1B**. While absolute HS does become small, the most important, *relative* heteroplasmy change may remain high, though estimates in these regions are less certain.

Significance. From the clinical perspective, wave-shaped selection impacts the prognosis and decisions for families affected by mtDNA diseases. From the fundamental perspective, it provides insight into the dynamics of mtDNA mutation in the germline and in the population. In **Fig. 1**, horizontal blue and red arrows represent the direction of expected changes of the heteroplasmy with time/generations. In the case of wave-shaped selection (**Fig. 1B**), a great majority of nascent low-fraction mutations will converge back to zero and vanish. However, due to random intracellular genetic drift, some mutations will, occasionally reach the threshold of positive selection (vertical red dotted line). Then they will be expanded by positive selection to higher, potentially detrimental levels, and become prone to downstream removal by selection on the cell or individual level. In this way, the wave-shaped selection may help to prevent the spread of detrimental mutations into the population and in the species. In contrast, if the descending selection profile (Fig 1A) was correct, nascent detrimental mutations would have been propelled to higher, but not as detrimental heteroplasmy levels, maximizing their spread in the population (**Suppl. Note 2**).

Abstract: The shift of the level of disease-causing mtDNA mutations (heteroplasmy) from mother to child is typically negatively correlated with the mother's heteroplasmy (H_m). In other words, mothers with low H_m tend to have children with a higher mutation level (H_{ch}) than their own. In contrast, mothers with high H_m typically see a decrease in heteroplasmy in their children. This peculiar trend has been commonly interpreted as a result of a descending germline selection profile, i.e., positive selection at low H_m, gradually turning negative at high H_m. Here we demonstrate, however, that the negative correlation is mostly driven by RTM, or 'Regression To the Mean', a classical statistical bias. We further show that RTM can be nullified by using the average between the mother's and child's heteroplasmy, as a new variable, instead of the commonly used mother's heteroplasmy in blood. Additionally, we demonstrate that mother/child average is a better proxy of the actual *germline* heteroplasmy. Moreover, the elimination of RTM revealed a previously hidden wave-shaped HS-profile (positive mother-to-child shift at intermediate average mother/child heteroplasmy, decreasing towards high and low average heteroplasmy). In confirmation of this finding, we show that simulations that involve both wave-shaped HS-profile and RTM, reproduce the observed patterns of inheritance of mtDNA mutations in unprecedented detail. From the health care perspective, the uncovering of the wave-shaped HS-profile (and the removal of the RTM bias) are crucial for millions of families affected by mtDNA disease. From the fundamental perspective, the wave-shaped profile offers a novel understanding of the germline dynamics of mtDNA and a novel potential mechanism that prevents the spread of detrimental mtDNA mutations in the population.

Abbreviations/conventions:
H_m – *heteroplasmy in mother's blood*, **H_{ch}** – *heteroplasmy in child's blood;* **HS** = $H_{ch} - H_m$ *heteroplasmy shift.*
HS(H_m) - heteroplasmy shift as a function of mother's heteroplasmy. The syntax in HS (H_{ch}), HS($(H_m+H_{ch})/2$), and H_{ch} (H_m) carries the equivalent meaning.

Introduction

mtDNA is present in many copies per cell, so mtDNA mutations are uniquely positioned for effective selection within cells, including germ cells. Also, because mitochondria are intimately involved in cell death and proliferation, mtDNA mutations are poised to affect germ cell attrition and proliferation. Collectively, these processes are thought to result in germline selection which has a major impact on the transmission of devastating mtDNA-based diseases, and, more generally, on the penetration of detrimental mtDNA mutations into populations and species. Germline selection has been actively discussed as a key means of eradicating of detrimental mutations since it was demonstrated that mtDNA mutations may be subject to negative germline selection (Fan et al. 2008; Stewart et al. 2008). On the other hand, the persistence of certain disease-causing mtDNA mutations in the human population hinted that detrimental mtDNA mutations may be, counterintuitively, under *positive* selection, as often proxied by the heteroplasmy shift (HS), i.e. the difference between the child's and the mother's heteroplasmy (See **Suppl. Notes 1 and 2** for cautions). For example, (Otten et al. 2018) observed that levels of the 8993T>G mutation tended to increase in the offspring (positive HS). Some of us (Fleischmann et al. 2021), and then Zhang et al. (H. Zhang et al. 2021), also reported positive germline selection of 3243A>G, the most prevalent disease-causing mutation and a few other inherited pathogenic mutations.

The overall positive or negative selection does not tell the whole story, however. As illustrated in **Fig. 1**, the precise shape of the mutation's "HS profile", i.e. heteroplasmy shift as a function of heteroplasmy, critically affects the heteroplasmy changes with time and the mode of inheritance of a mutation and its impact on future generations and the population/species as a whole. The question of how germline selection in the germline depends of the heteroplasmy level has been addressed in several studies. Zhang et al. reported strongly *descending* HS profiles for several inherited pathogenic mutations (H. Zhang et al. 2021). In all cases, heteroplasmy shift was positive at *lower* heteroplasmy, and decreased, eventually turning negative, at higher heteroplasmy (e.g., the profile for 3243A>G mutations is shown in Fig 1A). Zhang et al. concluded that it was "likely that the positive selection at lower heteroplasmy levels counterbalanced the negative selection at higher levels". We also have previously reported positive selection at low heteroplasmies and negative heteroplasmy shift correlation in m3243A>G, and proposed a similar, 'naïve' explanation at a conference (Khrapko 2019). This result, however, kept worrying us, primarily because the effect appeared unnaturally strong, and also the increase of the effect with decreasing heteroplasmy did not make biological sense. We, therefore, never published that observation is a journal and kept asking whether the apparent descending HS profile might have been a result of an error and sought to rectify the approach.

Analysis of the m3243A>G transmission requires compensating for life-long systematic changes of heteroplasmy in blood (Rajasimha, Chinnery, and Samuels 2008), (Grady et al. 2018). In hopes to improve the adjustment, we used the child's heteroplasmy instead of the mother's as a potentially more reliable reference because H_{ch} is expected to be developmentally 'closer' to the sought-after germline heteroplasmy and thus required a smaller and therefore more robust adjustment. This approach confirmed positive selection in the m3243A>G (Fleischmann et al. 2021), but, shockingly, the heteroplasmy shift profile was *inverted* and became ascending, i.e., the shift tended to be low/negative at low child's heteroplasmy and to increase towards high child's heteroplasmy. This apparent discrepancy was surprising because the child's and mother's heteroplasmies are correlated with each other, and from a biological standpoint, should not correlate with mtDNA transmission or selection in opposite ways. We therefore suspected that an artifact was skewing one or both approaches. Here we demonstrate that this is indeed an artifact i.e., the classical 'regression to the mean' (RTM) effect known for about 150 years (Galton 1886). We then show that RTM can be canceled and discuss the significance of the 'true' germline selection profile that becomes apparent after the removal of RTM (**Fig. 1**)

Results

The conventional negative correlation between the heteroplasmy shift and somatic heteroplasmy does not reflect the germline selection profile.

As discussed in the Introduction, previous studies posed a controversy: the HS profile that, by the 'naïve' interpretation, is expected to represent the germline selection profile, appears to change from descending to ascending depending on whether mother's (Khrapko 2019), (H. Zhang et al. 2021), or child's (Fleischmann et al. 2021) heteroplasmy was used as the reference. This was alarming because it appeared to imply that HS cannot be used to measure of germline selection. Also, it called for an explanation of such an extraordinary controversy.

First, we confirmed the existence of the controversy by repeating the mother-centered (HS(H_m)) and the child-centered analyses (HS(H_{ch})) using exactly the same dataset. For this purpose we used one from (H. Zhang et al. 2021), such that the only difference was in the use of either mother's, or child's heteroplasmy as reference. The results of the corresponding regression analyses are presented in **Fig. 2b and 2c**, respectively, and they fully confirm our concern: the two correlations are essentially symmetrical with opposite slopes. We also performed correlation analyses on other mutations for which extensive datasets are available, i.e., m8993T>G, m11778G>A, and m8344A>G using the data from (H. Zhang et al. 2021) for direct comparison with previous outcomes. The results are presented in supplementary **Fig. S2, a&d, b&e and c&f,** correspondingly. The results are qualitatively the same as for m3243A>G, which confirms that the observed opposite direction of slopes is a general phenomenon, not limited to the m3243A>G mutation.

Next, we verified that the opposite HS(H_m) and HS(H_{ch}) slopes indeed rejected the 'naïve' interpretation of the descending HS(H_m) profile as evidence of descending germline selection profile. To this end, we showed, both analytically and by a numerical simulation (Supplemental Fig. S3), that if germline selection profile were descending, then heteroplasmy shift would have a strong *negative* component in the correlation *both* with mother's *and* (even more so) with child's heteroplasmy, which directly contradicts the observations in Fig. 2c and Fig. S2, and therefore decisively rejects the hypothesis that a descending HS profile means a descending germline selection profile.

'Regression to the mean' (RTM) drives both the negative HS(H_m) and positive HS(H_{ch}) correlation.

In search of a phenomenon that could account for both negative HS(H_m) correlation AND positive HS(H_{ch}) correlation, we noted that negative correlations between HS and H_m in 3243A>G and other mutations (**Fig. 2d&g)** are highly reminiscent of the "regression towards mediocrity" phenomenon, first described in 1886 by Sir Francis Galton ((Galton 1886), *Fig. a* therein). This statistical bias, now called "regression towards mean" (RTM) refers to the tendency of parents who are 'extreme' with respect to a quantitative heritable trait (e.g., height) to have children who are closer to the population mean. The primary driver of the RTM effect is the non-inheritable variance of the trait. Extreme parents' height is most likely due to a synergic combination of the extreme genetic and extreme non-genetic variance. The offspring most likely will lack the extreme non-genetic part, and thus will appear in most cases to converge to the population average (Barnett 2004). This tendency naturally results in a negative correlation between the level of the trait in the parents and the parent-to-child shift, just like we see with heteroplasmy shift. RTM is symmetrical with respect to the parent/child change. Indeed, if a child is extremely tall, it is most likely due not only to genetic influence, but also to nongenetic influence that may not be shared with parents, so the parent(s) are likely to 'regress to the mean'. Thus the RTM-driven correlation between HS and child heteroplasmy must be *positive*, i.e., opposite to that between HS and Hm, and exactly as observed in the real-world mtDNA inheritance data. Thus, RTM has the potential to explain the puzzling trends in the mtDNA inheritance.

First, we explored the behavior of the RTM effect on simulated data resembling the mtDNA inheritance dataset. We asked whether the RTM effect alone (i.e., RTM in the absence of germline selection) can account for the observed negative correlation between HS and H_m. We started with the 'exact transmission' model (child inherits mother's heteroplasmy level), in which H_{ch} is equal to H_m and both are uniformly distributed from 0 to 1. We then added gradually increased Gaussian variance to match the variance of the experimental data (see **'Methods', 'RTM-only simulation'**). As discussed below in **Figure 3**, according to our biological interpretation, this variance is comprised of measurement error and variance generated in the somatic and germline bottlenecks. As standard deviation of the added variance in the simulation increased (0.1 to 0.3), the correlation between simulated H_{ch} and simulated H_m, expectedly, became weaker. The slope of H_{ch}(H_m) steadily decreased and the y-intercept increased (**Fig. S1**, top row, left to right). We thus used the comparison of the slope and the intercept to those of the experimental data as the criterion of the fitness of the model. The best fit variance (SD~0.24) was determined by comparing simulations at various SDs (see **Methods**). We then assessed the magnitude of the RTM effect in this 'best-fit' simulated dataset and compared it to the correlation of HS(H_m) and HS(H_{ch}) in the m3243A>G experimental dataset. Reassuringly, as shown in **Figure 2** (**b** vs. **f** and **c** vs. **g**), the two pairs of correlations (the simulated one and the experimentally observed one) are very similar. Thus, a realistic level of random variance can produce HS(H_m) and HS(H_{ch}) correlations similar to those observed experimentally. Therefore, these observed HS(Hm) and HS(Hch) correlations may be entirely spurious, not related to selection. This discovery implies that nullification of the RTM bias may reveal the residual 'true' germline selection profile.

Symmetrical (H_m+H_{ch})/2 variable cancels RTM and reveals an underlying wave-shaped germline selection profile.

As for nullifcation of RTM, we noted that because RTM-induced correlations have opposite signs depending on whether H_m or H_{ch} were used as the variable (**Fig. 2f** vs. **Fig. 2g**), they should cancel each other if the 'symmetrical' composite variable we used, such as (H_m+H_{ch})/2. **Fig. 2h** confirms this prediction: there is no correlation between HS and (H_m+H_{ch})/2 in the RTM-only model. Additional reason for the use of (H_m+H_{ch})/2 is that it is more

justified biologically than the conventionally used H_m measured in blood. Naturally, germline selection should depend on heteroplasmy in the germline, where selection takes place, not in the blood. As illustrated in **Fig. 3**, germline heteroplasmy is best approximated by $(H_m+H_{ch})/2$ (also see Discussion). Thus, we used the $(H_m+H_{ch})/2$ variable to cancel RTM and more appropriately represent the selection profile (**Fig. 2d**). Indeed, there is no significant linear trend in the experimental data plotted this way (**Fig. 2d,** black line**)**. Intriguingly, we also noted an excess of positive HS measurements at intermediate values of $(H_m+H_{ch})/2$. We therefore attempted to fit the data using quadratic regression, which indeed resulted in a highly significantly better fit (**Fig. 2d**, blue line). Reassuringly, there was no detectable quadratic component in the RTM-only simulated data (**Fig. 2h**, blue line). 4th power regression (red in **Fig. 2d**) resulted increase of R^2 compared to quadratic regression. Further increase of power

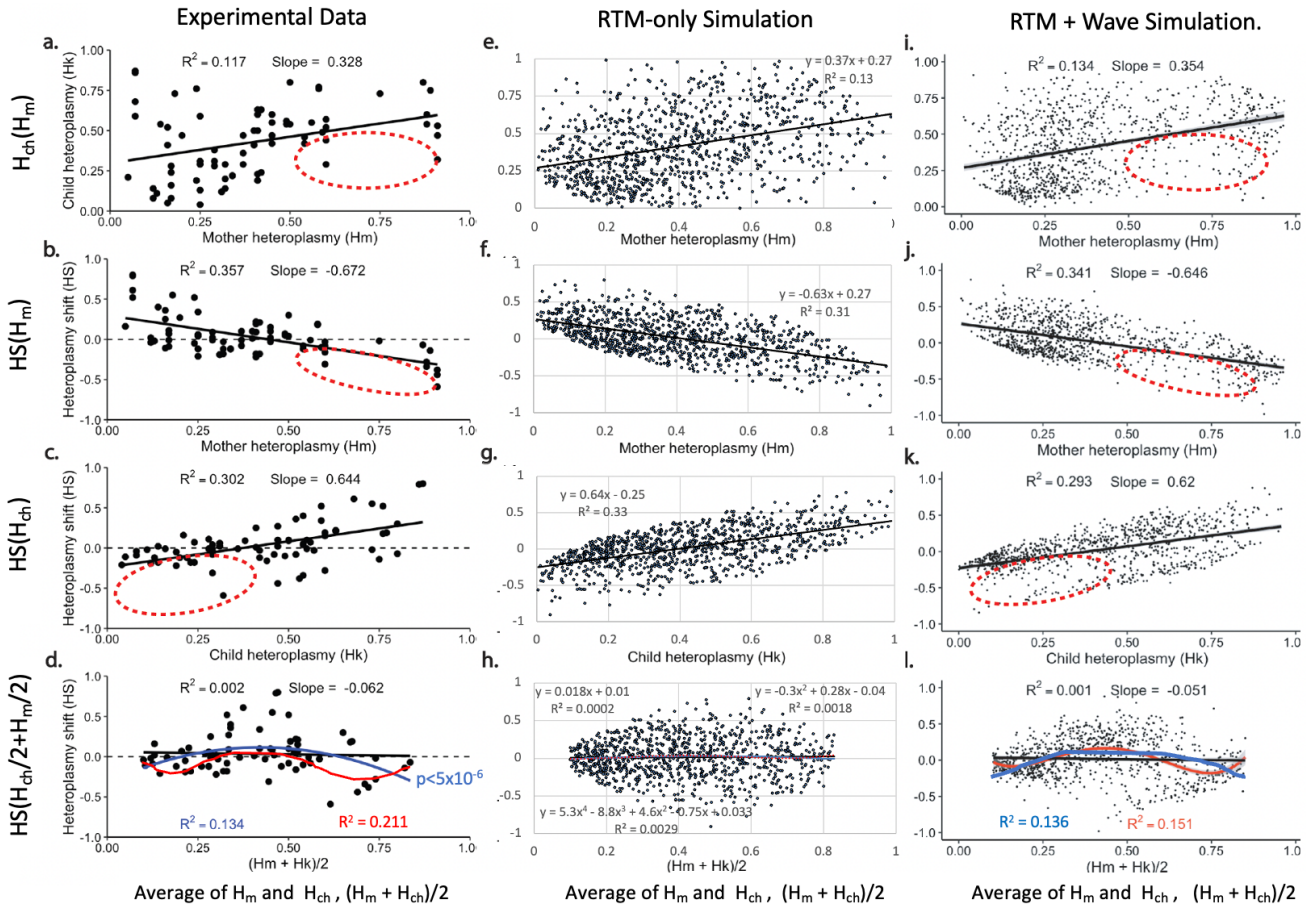

Figure 2. **Regression analysis of experimenlal and simulated data demonstrates that germline selection follows a "wave-shaped profile"**.
Data. *Left column, **(a-d)***: the experimental data - m3243A>G mother-child inheritance (public dataset, see methods for details). *Central column, **(e-h)***: RTM-only simulation: Gaussian variance (SD=0.24) was added to the 'exact transmission' dataset $\{H_m=H_{ch}\}$, $(0< H_m,H_{ch}<1)$. *Right column, **(i-l)***: full simulation, i.e., exact transmission dataset with added Gaussian variance (0.135) AND the wave-shaped selection profile (see Methods for details).
Interpretation: negative $HS(H_m)$ correlation (**b**) previously suggested that m3243A>G mutation was under germline selection that decreases from positive selection at low Hm, to negative selection at high Hm (see **Fig. 1A**). This hypothesis, however, is rejected, because it predicts that HS also decreases with Hk (Fig.S3 and discussion there), in contradiction with the observed positive correlation (**c**). Opposite correlations with H_m and H_{ch} are predicted if the data is affected by the "regression to the mean" bias (RTM), which is driven by data variance (**Fig. S1**). Indeed, our simulations show that experimentally observed correlations (**a-c**) may be fully accounted by the pure RTM (**e-g**). RTM Because RTM changes sign when H_k as a variable is changed to H_m (**f** vs. **g**), it follows that RTM can be nullified by the use of the symmetrical variable $(H_m+H_{ch})/2$, as confirmed in (**h**). In support of the hypothesis that $HS(H_m)$ in experimental data is driven by RTM, this correlation was reduced to insignificant by the use of the $(H_m+H_{ch})/2$ variable, as shown in (**d**). However, in the experimental dataset, cancellation of RTM revealed a highly significant ($p<6x10^{-5}$) residual non-linear data skew, which is efficiently described by a quadratic (blue) or 4th-order (red) function (**d** , see also **Fig. S4**). This residual skew is, as expected, not present in the RTM-only simulation (**h**), which thus serves as an effective control. Accordingly, to advance the model, we complemented the RTM-only simulation with 'wave-shaped selection', i.e., the 4th order function from (**d**); The RTM+Wave simulation (right column (**i – l**)) correctly reproduces the residual 4th order regression (**l**). Moreover, it required the addition of only half of the variance needed for RTM-only simulation, because the added wave-shaped selection strengthened, synergistically with RTM, the $HS(H_m)$ and $HS(H_{ch})$ correlations. Finally, RTM+Wave model reproduced the marked inhomogeneity of the experimentally observed datapoint 'clouds' (**a-c**). In particular, voids (red ellipses) in the simulated clouds appear reminiscent of the simlar irregularities in the experimental datapoint clouds. Statistical analysis of these similarities is complicated and is ongoing. We conclude that m3243A>G data distribution is mostly shaped by a combination of the wave-shaped germline selection and the RTM effect.

to 5th and 6th added no additional improvement of the fitness (**Fig. S4**). We, therefore, chose 4th power regression as our standard analysis of the HS($(H_m+H_{ch})/2$) data plots. We postulate that this residual wave-shaped profile represents the true selection in the germline.

Model that combines RTM and the wave-shaped selection precisely predicts experimental HS trends.

The discovery of the residual wave-shaped selection in the experimental data implied that our RTM-only model that lacked such a residual (Fig. 2h) was incomplete. We therefore sought to incorporate the wave-shaped selection profile into the model. The 'natural' way to achieve this is to use an "input" selection curve to generate the simulated pairs of mother-child germline heteroplasmy dataset. To these selection-only data pairs, we added Gaussian variance in the same way as we did in the RTM-only simulation (see **Methods**). This approach is identical to the RTM-only simulation except here we used the selection-only data instead of the exact transmission data used in the RTM-only approach. To evaluate the model, we subjected the resulting simulated data to the regression analysis, identical to that used for experimental data and RTM-only simulation (Fig. 2). The criterion of success was (as in RTM-only) the similarity of the slopes and Y-intersects of regression lines of the simulated data to those of the m3243A>G experimental inheritance data (**Fig. 2**, left column). Additionally, we assessed if the model reproduces the the shape and amplitude of the observed residual wave-shaped curve (the "output" selection curve).

We started with a pilot simulation that used, as the input curve, intuitively, the experimentally observed m3243A>G residual wave-shaped 4th power regression curve (**Fig. 2d)** and as the input variance, the variance of the best fit RTM-only model (Fig. 2i-l). This pilot simulation resulted in excessively steep regression slopes, both HS(H_m) and HS(H_{ch}) and excessively shallow slope of the Hk(Hm) correlation **(Suppl. Fig. S5 b, c, and a,** correspondingly). We concluded that (1) the addition of the selection into the model exacerbated the effect of RTM. Therefore the correlations in the experimental data must result from synergistic interaction between RTM and germline selection. At the same time, (2) the residual wave-shaped "output selection" curve was 'dampened', compared to the input curve (**Suppl. Fig. S5d**). This dampening effect is an expected result of added random noise. Thus, the real selection curve must be an augmented derivative of the experimentally observed residual curve shown in Fig. 2d.

Based on these two conclusions we optimized the model by (1) decreasing the added variance and (2) augmenting the added selection curve. We performed several iterations of optimization which greatly improved the simulation. Reassuringly, optimization simultaneously improved the fit along all the criteria: the HS(H_m) and HS(H_{ch}) slopes and Y-intersections, the R^2 of correlations, and the shape of the 'output' residual selection curve, and eventually precisely satisfied all optimization criteria.

The results of the optimized simulation are shown in **Fig. 2i-l** (right column). Additionally, simulation appears to reproduce the otherwise mysterious 'voids' in the datapoint clouds (shown by ellipsoids in **Fig. 2**). Furthermore, the RTM-plus-selection simulation accounted for otherwise puzzling disparity between HS(H_m) and HS(H_{ch}) slopes, which under no conditions could be reproduced in RTM-only simulations (see **Supplemental Methods** for more detail). Whereas the statistical significance of 'the voids' and 'the disparity' is difficult to assess, their mere presence collectively boosts our confidence in the simulations. We conclude that the wave-shaped selection profile model fully accounts for the key features of the m3243A>G dataset which supports the hypothesis that the germline selection of these mutations indeed follows such a profile. As a note of caution, our analysis has not excluded the possibility that other models could equally reproduce the dataset's properties.

Wave-shaped selection is a general phenomenon: analysis of other disease-causing mtDNA mutations.

To explore the generality of the wave-shaped selection profile, we performed regression analysis of other human mtDNA mutations for which rich enough datasets are available: m8993T>G, m11778G>A, and m8344A>G using data from Zhang et al. to ensure compatibility of the results. The analyses are shown in the Supplement, **Fig. S2**. Similar to m3243A>G and as expected, all mutations show strong negative HS(H_m) correlations (**Fig. S2, a-c**). Also, similarly to m3243A>G and to the RTM-only simulation, the correlation of HS(H_{ch}) is positive (**Fig. S2, d-f**), which suggests the presence of the RTM effect. And, finally, m8993T>G and m11778G>A also show a wave-shaped selection profile when plotted against $(H_m+H_{ch})/2$ (**Fig. S2, g, h**). Additionally, both of these mutations show overall more positive germline selection than m3243A>G (average HS across all heteroplasmy levels is more positive). Interestingly the last mutation, m8344A>G does not show an arch, but a weak monotonous *increase* of HS with $(H_m+H_{ch})/2$ (**Fig. S2i**). This is the opposite of the inference for this mutation using H_m as the independent variable.

This difference between m8344A>G and other three mutations may imply fundamental dissimilarities between the mechanisms of germline selection. From methodological point, this observation reassures us that the arched shape observed in other mutations is not an artifact inherent to our analysis, but a true biological phenomenon. This is effectively a negative control in the experimental data, which adds to the negative control in the simulated data without selection (i.e. **Fig. 2h**), though more data are needed for definitive conclusions.

Discussion

Possible mechanisms underlying the 'wave-shaped' selection profile

It is tempting to speculate regarding the possibe mechanism(s) responsible for the 'wave-shaped' selection profile which was uncovered by removing the RTM effect. It appears likely that the complexity of the profile is a result of a superposition of multiple processes, some of which are responsible for purifying selection, and some for positive selection. Indeed, there is substantial

literature both on positive (Holt, Speijer, and Kirkwood 2014; Kowald and Kirkwood 2018) and negative (Gottlieb et al. 2021) selection of mitochondria and mitochondrial mutations. Importantly, purifying selection can proceed on a single mitochondrion level, for example, by a mitochondrion-autonomous negative feedback loop such as the PINK1-Larp loop (Y. Zhang et al. 2019). This implies that purifying selection may be operational at very low mutant fractions, which potentially accounts for the prevalence of negative selection in the left extreme of the selection profile. There are very little data available with low H_m values, however, and definitive conclusions about germline selection at low heteroplasmy would be premature.

Purifying negative selection on a single mitochondrion level mentioned above (Y. Zhang et al. 2019) may be expected to counteract positive selection that we observe at higher heteroplasmy levels. This effect, however, appears to be not strong enough as detrimental mtDNA mutations are known to be under positive selection in tissues as diverse as muscle (Nicholas et al. 2009), choroid plexus (Campbell et al. 2012) and colon (Taylor et al. 2003). One therefore must assume that mitochondrion-autonomous purifying selection may either cease at higher mutant fractions and/or be overcome by positive selection. This assumption fits well with the wave-shaped selection profile, though specific mechanisms explaining positive selection are still a matter of debate (Holt, Speijer, and Kirkwood 2014), (Kowald and Kirkwood 2018). Note that at intermediate heteroplasmy levels, positive selection does not necessarily need to proceed at a single mitochondrion level. As heteroplasmy levels exceed physiological threshold (Konstantin Khrapko and Turnbull 2014), the physiology of the entire cell may change, which, for example, may make the cell more prone to proliferation (Smith et al. 2020). Finally, at even higher mutant fractions, (as has been repeatedly proposed by many researchers in the field) detrimental mutations may become progressively more toxic to the cell and cause slowdown of proliferation or active removal of highly mutant germ cells cells (e.g. by attrition (Fan et al. 2008)), or by embryo demise.

Biological justification of the use of the $(H_m+H_{ch})/2$ variable

In this study we used the symmetrical $(H_m+H_{ch})/2$ variable to cancel the RTM effect. There is another compelling reason to use $(H_m+H_{ch})/2$ as an independent variable instead of the H_m, which is traditionally used to describing germline selection of mtDNA. Note that there is no consensus regarding the precise mechanism and location of mtDNA bottleneck, which is currently variably described by several competing models (Cao et al. 2007; Cree et al. 2008; K. Khrapko 2008; Lee et al. 2012; Wai, Teoli, and Shoubridge 2008). Similarly, there is little consensus about the location, mechanism, and even direction of germline selection. Nevertheless, most models (Fleishmann et al. 2021; Floros et al. 2018; H. Zhang et al. 2021) postulate that selection takes place sometime during and/or after the embryonic mtDNA bottleneck (Cree et al. 2008). Granted, selection process must be controlled not by the mother's heteroplasmy in blood (H_m), but by heteroplasmy in germ cells around the bottleneck. As schematically illustrated in **Fig. 3**, blood heteroplasmy is separated from the 'around-bottleneck' heteroplasmy by changes in heteroplasmy during blood development and the lifelong cell dynamics in the blood (Rajasimha, Chinnery, and Samuels 2008), (Franco et al. 2022; Grady et al. 2018), which collectively represent a 'somatic bottleneck' (Barrett et al. 2020). Given that these random changes take place in blood samples from both mothers and children, $(H_m+H_{ch})/2$ must be a better proxy of heteroplasmy level at the point where selection is expected to take place than the conventionally used mother's heteroplasmy in blood.

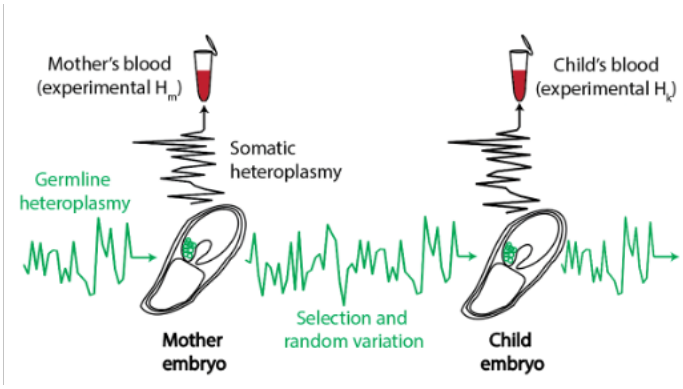

Figure 3. $(H_m+H_{ch})/2$, the average of mother's and child's heteroplasmy in blood, is a better proxy of heteroplasmy level determining selection than H_m. The mother's and the child's blood heteroplasmy levels (H_m and H_{ch}) are typically used as proxy estimates of mother's and child's germline heteroplasmy in human germline selection studies. These estimates are subject to natural error / variance caused by random processes taking place during blood development and later due to blood composition changes (depicted by the blue zig-zags, sometimes dubbed 'somatic bottleneck'). Heteroplasmy of the germline itself also changes as primordial germ cells proliferate and progress through mtDNA bottleneck (green zig-zag). Germline selection has been proposed to proceed in PGCs (Floros 2018), (Fleischmann 2021), or in oocyte (Zhang 2021). The site of germline selection has to be somewhere between the points in the mother's and the child's embryos where germ cells are separated into an isolated lineage. The scheme shows that commonly used mother's heteroplasmy H_m, is a rather suboptimal variable to characterize the germline selection process: H_m, as well as and child's heteroplasmy, H_{ch} are 'developmentally distant' from the region where germline selection presumably proceeds, and where heteroplasmy level is likely to influence selection. It therefore appears that, most likely, the average mother/child heteroplasmy, $(H_m+H_{ch})/2$ is a better variable to characterize germline selection than H_m.

Proposed biological significance of the wave-shaped selection profile.

Negative or zero selection in the lower heteroplasmy segment (left extreme of the wave, **Fig. 1**) is expected to prevent nascent mutations (which are initially necessarily ocurr at a very low fraction) from expansion. Most of them are destined to disappear in the nearest cell generations, largely due to intracellular random genetic drift (Coller, Bodyak, and Khrapko 2002). However, drift is expected to propel a small proportion of nascent mutations to intermediate fractions. These mutations potentially pose the

danger of being spread into subsequent generations and further into the population. With the wave selection profile, these mutations will be further enriched to even higher levels by the positive selection that prevails at intermediate heteroplasmy levels. The resulting individuals (or oocytes, or embryos) with a detrimental mutation at high heteroplasmy levels will likely be unfit and therefore removed from population by Darwinian selection (or oocyte attrition, or embryo demise), before mutation is spread further. Our preliminary simulations imply that this strategy may indeed be efficient in protecting the genetic pool of the population under realistic assumptions (in preparation). In contrast, with the continuously descending selection profile (grey line in **Fig. 1A**), positive selection at low heteroplasmy will increase the proportion of nascent mutations that reach higher fractions, which means increased mutational pressure. Furthermore, mutations that reach intermediate fractions are not pushed to highly detrimental levels. Instead, they are expected to converge to intermediate level both from below and from above. Thus, they are expected to remain at mildly detrimental levels which are most dangerous as far as transmission to offspring and contaminating of the population's genetic material is concerned.

Future directions

We note that mitigation of RTM by using the $(H_m+H_{ch})/2$ variable is just the first, though likely a major, step in elucidating of the selection profiles based on mother/child heteroplasmy shift data. One of the results of this study was to identify RTM as a major bias in analysis of mtDNA inheritance and to find a way to factor it out. We recognize, however, that additional, finer, adjustments may be needed to establish the precise residual selection profiles with even higher accuracy. There are two aspects that we anticipate will need to be addressed. The HS-based selection analysis considers absolute changes of heteroplasmy, whereas relative changes better reflect the selection intensity. Consideration of relative changes is particularly important at low heteroplasmy levels. The h' measure (**Ref**) ideally represents intensity of selection in the entire range of heteroplasmy levels, however,

Methods

Data:

Regression analysis

To perform the analyses of the effect of regression to the mean, for each of the experimental and simulated mother-child inheritance datasets (i.e. any collection of (H_m,H_{ch}) pairs of (mother, child) heteroplasmy measurements) we first calculated, for every mother-child pair, heteroplasmy shift $HS= H_{ch} - H_m$, and plotted heteroplasmy shifts as a function of mother's heteroplasmy $HS(H_m)$, child heteroplasmy $HS(H_{ch})$, and also as a function of the 'symmetrized', average mother/child heteroplasmy, $HS((H_m+H_{ch})/2)$. Linear and polynomial regression analysis of the data was performed using Excel's built-in analysis tools.

***Note**: all heteroplasmies used in this figure (Hm, Hk) are measured or simulated as heteroplasmies in blood. The graphs in the last row, however, represent heteroplasmy shift in the germline because $(H_m+H_{ch})/2$ represents heteroplasmy in the germline.*

RTM-only simulation (**Fig. 2** middle column, and **Fig. S1**)

In the RTM-only simulation is based on the exact transmission model, i.e. we assumed that the child inherits its mother's heteroplasmy without change ($H_m = H_{ch}$). This model ensures the absence of any systematic selection and no variance. Specifically, we started with 10,000 pairs of equal values ($H_m = H_{ch}$) sampled uniformly between 0 and 1 (i.e. sampled with a 0.0001 step). To emulate the RTM effect, we added variance to this model by adding to each mother and child heteroplasmy value a number randomly drawn from a Gaussian distribution. We performed a series of such simulations using various standard deviation values to define the Gaussian distribution (the results of simulations with SD=0 (the original undisturbed model) and datasets with added Gaussian noise with SD=0.1, SD=0.2, and SD=0.3 are shown in **Fig. S1**. Data pairs in which one or both of the simulated mother/child heteroplasmy values was outside the 0.1-0.85 range were deleted. Note that for fairness of comparison, such mother/child pairs were also deleted from the experimental 3243 Zhang dataset.

Additionally, to avoid potential biases related to the difference between the uniform distribution of the simulated data and the uneven distribution of experimental data points we emulated the experimental distribution of data points in our simulations and picked the simulated data points from the experimental distribution.

As expected, the slope and R^2 of the linear regression between H_m and H_{ch} systematically decreased as standard deviation of the added Gaussian variance was increased. At the same time, also as expected, the strength of the RTM effect (represented by the slopes of linear regressions of the distributions $HS(H_m)$ and $HS(H_{ch})$) increased in absolute terms, but in opposite directions (**Fig. S1** second and third row, correspondingly). We chose the slope and R2 of the linear regression between H_{ch} and H_m as a criterion to select the simulation that best fitted the experimental m3243A>G dataset. The addition of variance using a Gaussian distribution with a standard deviation of 0.275 ensured best fit (in the simulation a slope of 0.35 and R^2 of 0.12, vs a slope of 0.33 and R^2 of 0.12 in the experimental data – see **Fig. 2a** and **Fig. 2b**). We then subjected the simulated dataset with an SD of 0.275 to the 'RTM analysis' described above and compared the result to that of the Zhang dataset of 3243 mutation inheritance. The resulting plots show close similarity between the experimental and simulated datasets with respect to all linear correlations (**Fig. 2**, compare plots on the left column to those in the center column). Figure 2 (center column) is a representative subsample of the simulated dataset, which was obtained by down-sampling the simulation to 85 datapoints for easy visual comparison to the experimental data. The regression parameters shown in center column pertain to the full simulation (10,000 datapoints).

RTM+Wave simulation (**Fig. 2**, right column) .

To assess the combined effect of wave-shaped germline selection and RTM, we first generated a 10,000 – strong set of data pairs representing the systematic selection in the germline. This dataset consisted of $\{H_m+H_c)/2, HS((H_m+H_c)/2)\}$ pairs of values which followed an appropriate wave-shaped curve (e.g., the 4th order curve in **Fig. 2d**, or adjusted curves in the optimization simulations). According to our scenario, this systematic heteroplasmy change in the germline was then succeeded with random variance as heteroplasmic mtDNA was distributed into the blood cells (**Fig. 3**). Consequently, we first converted the germline heteroplasmy level $H_m+H_c)/2$ into the corresponding heteroplasmy levels in mother and child, $\{H_m, H_{ch}\}$ and then added the appropriate random variance to both H_m and H_{ch}. Such conversion is possible by solving a system of linear equations for each $\{H_m+H_c)/2, HS((H_m+H_c)/2)\}$ pair. Then the resulting 'noisy' dataset was subject to the regression analysis shown in Fig 2 and described in the 'regression analysis' section above.

In the first pilot simulation, we used as a first approximation the input parameters the experimentally observed residual arched profile (Fig 2d, red curve) and variance of the RTM-only simulation (**Fig. 2e-h**). The first pilot simulation, resulted in excessively strong $HS(H_m)$ correlation in the simulated data (the regression lines, both $HS(H_m)$ and $HS(H_{ch})$ were steeper than in the experimental dataset (**Fig. S##**. **b** and **c.** Also, the output residual regression curve was 'dampened', i.e. whereas the overall shape of the curve was unchanged, the minima and the maxima were reduced about 1.5-fold. (**Fig. S##**. **d**). The mechanism of this effect is similar to the deterioration of a sharp signal peak in a noisy environment. Thus the residual regression curve of the experimental m3243A>G in **Fig. 2d** is a blunted derivation of the real germline selection profile. We therefore concluded that to reconstruct the original selection profile and to achieve a high-fit simulation, the standard deviation of the added variance must be reduced and the input wave-shaped curve must be augmented (i.e., the absolute values of the maximum and the minima must be proportionally increased compared to the experimentally observed residual curve). With that in mind, we performed several iterations of the simulations and determined that decreasing the standard deviation of the added variance to 0.21 and augmenting the wave-shaped curve 1.5 times ensures an optimized fit of the summary features of the m3243A>G experimental data. The results of the optimized simulation are presented in **Fig. 2,** right column.

Monte Carlo estimation of significance.

To determine whether the non-linear selection profile was a statistically significant finding, we determined the probability that the quadratic regression of the magnitude observed in the experimental m3243A>G data appears by pure chance in the absence of selection. We performed 100,000 random samplings of 85 datapoints each (to match the 85 ndataspoints in the experimental set) from the RTM-only simulated dataset and then counted the number of instances where the R^2 of the second order best-fit quadratic curve exceeded 0.134, which is the quadratic R^2 of the experimental m3243A>G dataset. There were six such cases, putting the p-value below $6x10^{-5}$.

Data availability

In this study we used the mtDNA mutation inheritance datasets published by Zhang et al., for the purpose of consistency. In this dataset, the m3243A>G data was corrected for the decay of heteroplasmy levels in blood with age.

References

Barnett, A. G. 2004. "Regression to the Mean: What It Is and How to Deal with It." *International Journal of Epidemiology* 34 (1): 215–20. https://doi.org/10.1093/ije/dyh299.

Barrett, Alison, Barbara Arbeithuber, Arslan Zaidi, Peter Wilton, Ian M. Paul, Rasmus Nielsen, and Kateryna D. Makova. 2020. "Pronounced Somatic Bottleneck in Mitochondrial DNA of Human Hair." *Philosophical Transactions of the Royal Society B: Biological Sciences* 375 (1790): 20190175. https://doi.org/10.1098/rstb.2019.0175.

Campbell, G. R., Y. Kraytsberg, K. J. Krishnan, N. Ohno, I. Ziabreva, A. Reeve, B. D. Trapp, et al. 2012. "Clonally Expanded Mitochondrial DNA Deletions within the Choroid Plexus in Multiple Sclerosis." *Acta Neuropathologica* 124 (2): 209–20. https://doi.org/10.1007/s00401-012-1001-9.

Cao, L., H. Shitara, T. Horii, Y. Nagao, H. Imai, K. Abe, T. Hara, J. Hayashi, and H. Yonekawa. 2007. "The Mitochondrial Bottleneck Occurs without Reduction of mtDNA Content in Female Mouse Germ Cells." *Nature Genet* 39 (3): 386–90.

Coller, H. A., N. D. Bodyak, and K. Khrapko. 2002. "Frequent Intracellular Clonal Expansions of Somatic mtDNA Mutations: Significance and Mechanisms." *Ann N Y Acad Sci* 959 (April): 434–47.

Cree, L. M., D. C. Samuels, S. C. de Sousa Lopes, H. K. Rajasimha, P. Wonnapinij, J. R. Mann, H. H. Dahl, and P. F. Chinnery. 2008. "A Reduction of Mitochondrial DNA Molecules during Embryogenesis Explains the Rapid Segregation of Genotypes." *Nature Genet* 40 (2): 249–54.

Fan, W., K. G. Waymire, N. Narula, P. Li, C. Rocher, P. E. Coskun, M. A. Vannan, J. Narula, G. R. MacGregor, and D. C. Wallace. 2008. "A Mouse Model of Mitochondrial Disease Reveals Germline Selection

against Severe mtDNA Mutations." *Science* 319 (5865): 958–62.

Fleischmann, Zoe, Sarah J. Pickett, Melissa Franco, Dylan Aidlen, Mark Khrapko, David Stein, Natasha Markuzon, et al. 2021. "Bi-Phasic Dynamics of the Mitochondrial DNA Mutation m.3243A>G in Blood: An Unbiased, Mutation Level-Dependent Model Implies Positive Selection in the Germline." *bioRxiv*, January, 2021.02.26.433045. https://doi.org/10.1101/2021.02.26.433045.

Fleishmann, Zoe, Sarah J. Pickett, Melissa Franco, Dylan Aidlen, Mark Khrapko, David Stein, Natasha Markuzon, et al. 2021. "Bi-Phasic Dynamics of the Mitochondrial DNA Mutation m.3243A>G in Blood: An Unbiased, Mutation Level-Dependent Model Implies Positive Selection in the Germline." *bioRxiv*. https://doi.org/10.1101/2021.02.26.433045.

Floros, Vasileios I., Angela Pyle, Sabine Dietmann, Wei Wei, Walfred C. W. Tang, Naoko Irie, Brendan Payne, et al. 2018. "Segregation of Mitochondrial DNA Heteroplasmy through a Developmental Genetic Bottleneck in Human Embryos." *Nature Cell Biology* 20 (2): 144–51.

Franco, Melissa, Sarah J Pickett, Zoe Fleischmann, Mark Khrapko, Auden Cote-L'Heureux, Dylan Aidlen, David Stein, et al. 2022. "Dynamics of the Most Common Pathogenic mtDNA Variant m.3243A>G Demonstrate Frequency-Dependency in Blood and Positive Selection in the Germline." *Human Molecular Genetics* 31 (23): 4075–86. https://doi.org/10.1093/hmg/ddac149.

Galton, Francis. 1886. "Regression Towards Mediocrity in Hereditary Stature." *The Journal of the Anthropological Institute of Great Britain and Ireland* 15: 246. https://doi.org/10.2307/2841583.

Gottlieb, Roberta A., Honit Piplani, Jon Sin, Savannah Sawaged, Syed M. Hamid, David J. Taylor, and Juliana de Freitas Germano. 2021. "At the Heart of Mitochondrial Quality Control: Many Roads to the Top." *Cellular and Molecular Life Sciences* 78 (8): 3791–3801. https://doi.org/10.1007/s00018-021-03772-3.

Grady, John P., Sarah J. Pickett, Yi Shiau Ng, Charlotte L. Alston, Emma L. Blakely, Steven A. Hardy, Catherine L. Feeney, et al. 2018. "mtDNA Heteroplasmy Level and Copy Number Indicate Disease Burden in m.3243A>G Mitochondrial Disease." *EMBO Molecular Medicine* 10 (6): e8262. https://doi.org/10.15252/emmm.201708262.

Holt, Ian J., Dave Speijer, and Thomas B. L. Kirkwood. 2014. "The Road to Rack and Ruin: Selecting Deleterious Mitochondrial DNA Variants." *Philos Trans R Soc Lond B Biol Sci* 369 (1646).

Khrapko. 2019. "MtDNA Bottleneck against Dertrimental mtDNA Mutations: What Does It Do, and What It Does't." In . Moscow, Russia.

Khrapko, K. 2008. "Two Ways to Make an mtDNA Bottleneck." *Nature Genet* 40 (2): 134–35.

Khrapko, Konstantin, and Doug Turnbull. 2014. "Mitochondrial DNA Mutations in Aging." *Progress in Molecular Biology and Translational Science* 127: 29–62. https://doi.org/10.1016/b978-0-12-394625-6.00002-7.

Kowald, Axel, and Thomas B. L. Kirkwood. 2018. "Resolving the Enigma of the Clonal Expansion of mtDNA Deletions." *Genes* 9 (3): 126. https://doi.org/10.3390/genes9030126.

Lee, H. S., H. Ma, R. C. Juanes, M. Tachibana, M. Sparman, J. Woodward, C. Ramsey, et al. 2012. "Rapid Mitochondrial DNA Segregation in Primate Preimplantation Embryos Precedes Somatic and Germline Bottleneck." *Cell Reports* 1 (5): 506–15. https://doi.org/10.1016/j.celrep.2012.03.011.

Nicholas, A., Y. Kraytsberg, X. Guo, and K. Khrapko. 2009. "On the Timing and the Extent of Clonal Expansion of mtDNA Deletions: Evidence from Single-Molecule PCR." *Exp Neurol* 218 (2): 316–19.

Otten, Auke B. C., Suzanne C. E. H. Sallevelt, Phillippa J. Carling, Joseph C. F. M. Dreesen, Marion Drüsedau, Sabine Spierts, Aimee D. C. Paulussen, et al. 2018. "Mutation-Specific Effects in Germline Transmission of Pathogenic mtDNA Variants." *Hum Reprod* 33 (7): 1331–41.

Rajasimha, Harsha Karur, Patrick F. Chinnery, and David C. Samuels. 2008. "Selection against Pathogenic mtDNA Mutations in a Stem Cell Population Leads to the Loss of the 3243A→G Mutation in Blood." *The American Journal of Human Genetics* 82 (2): 333–43. https://doi.org/10.1016/j.ajhg.2007.10.007.

Smith, Anna L. M., Julia C. Whitehall, Carla Bradshaw, David Gay, Fiona Robertson, Alasdair P. Blain, Gavin Hudson, et al. 2020. "Age-Associated Mitochondrial DNA Mutations Cause Metabolic Remodeling That Contributes to Accelerated Intestinal Tumorigenesis." *Nature Cancer* 1 (10): 976–89.

Stewart, James Bruce, Christoph Freyer, Joanna L. Elson, and Nils-Goran Larsson. 2008. "Purifying Selection of mtDNA and Its Implications for Understanding Evolution and Mitochondrial Disease." *Nat Rev Genet* 9 (9): 657–62. https://doi.org/10.1038/nrg2396.

Taylor, R. W., M. J. Barron, G. M. Borthwick, A. Gospel, P. F. Chinnery, D. C. Samuels, G. A. Taylor, et al. 2003. "Mitochondrial DNA Mutations in Human Colonic Crypt Stem Cells." *J Clin Invest* 112 (9): 1351–60.

Wai, T., D. Teoli, and E. A. Shoubridge. 2008. "The Mitochondrial DNA Genetic Bottleneck Results from Replication of a Subpopulation of Genomes." *Nature Genet* 40 (12): 1484–88. https://doi.org/10.1038/ng.258.

Zhang, Haixin, Marco Esposito, Mikael G. Pezet, Juvid Aryaman, Wei Wei, Florian Klimm, Claudia Calabrese, et al. 2021. "Mitochondrial DNA Heteroplasmy Is Modulated during Oocyte Development Propagating Mutation Transmission." *Science Advances* 7 (50): eabi5657. https://doi.org/10.1126/sciadv.abi5657.

Zhang, Yi, Zong-Heng Wang, Yi Liu, Yong Chen, Nuo Sun, Marjan Gucek, Fan Zhang, and Hong Xu. 2019.

"PINK1 Inhibits Local Protein Synthesis to Limit Transmission of Deleterious Mitochondrial DNA Mutations." *Molecular Cell* 73 (6): 1127-1137.e5. https://doi.org/10.1016/j.molcel.2019.01.013.

Supplementary Note 1. Reasons for not using the transformed heteroplasmy measure ***h'***.

In this paper, we use heteroplasmy shift, (HS), as a proxy of the selection intensity. We appreciate that this is not the best approach. The most appropriate measure of the "selection intensity" imposed on a mutation is the **h'** measure, with the confusing name "transformed heteroplasmy", defined as:

$$h' = \ln (H_c(1 - H_m)/H_m (1 - H_c))$$ *(Wonnapinij et al 2010).*

Compared to the heteroplasmy shift, HS, "transformed heteroplasmy" ***h'*** addresses two problems of selection measurement:

First, it appropriately measures relative, not absolute changes in heteroplasmy. This distinction is most important at the low heteroplasmy end, where, say Hm=0.01 to Hc=0.02 heteroplasmy change is very small (0.01) by HS, and a very strong 2-fold increase per generation (actually Ln2).

Second, at the high end of heteroplasmy, the last small steps to homoplasmy look small even in the relative representation. For example, if Hm=0.98 to Hc=0.99 HS is only 0.01, but in fact, this change requires a very high "selection intensity" equal to the 0.01 to 0.02 change discussed above. And indeed, the h' in this case correctly yields ln2 as the logarithmic measure of selection per generation.

The downside of ***h'*** is that at the extremes of the heteroplasmy range, where it's most needed, it also becomes highly unstable with respect to any random variance in the data, as denominators become close or equal to zero. Therefore, ***h'*** becomes essentially dysfunctional as a measurement of selection in noisy datasets like the pathogenic mutations' inheritance datasets used in this study.

Supplementary Note 2. Justification of semi-qualitative conclusions drawn from the Heteroplasmy Shift (HS) analysis.

Heteroplasmy Shift, HS though it lacks the rigor of ***h'***, particularly at the extremes of heteroplasmy (suppl note 1), offers a sensible qualitative assessment of selection, and in particular, it's ability to identify the points where selection changes its sign is as good as of ***h'***.

Because the purpose of our analysis is not to precisely quantify the selection but rather to explain the observed patterns, it is sufficient to use the HS. In all situations where we make analogies between HS and "true selection", our comparisons are qualitative and limited to referring to the sign of selection, (such as in Figure 1, blue and red arrows), which is correctly assessed by HS.

Furthermore, the available data on 3243A>G is scarce at either extremes of the heteroplasmy range. So in fact the currently available data does not permit to make conclusions on whether selection exists and whether it is positive or negative below heteroplasmy ~10%. This unfortunately does not permit us to precisely explore what happens to inherited pathogenic mutations at the lowest heteroplasmy levels, right after their emergence (which is about 0.001, as a PGC contains about 1000 mtDNA molecules). Nevertheless, we can very definitely *compare* the predictions of the monotonously descending (Fig 1A) vs wave-shaped (Fig 1B) HS-profile and state (as we do) that the descending profile predicts that nascent detrimental mutations would have been

propelled to higher, but not as detrimental heteroplasmy levels, maximizing their spread in the population, whereas in the case of wave-shaped selection (**Fig. 1B**), a great majority of nascent low-fraction mutations will converge back to zero and vanish.

We must caution, however, against overinterpreting the wave-shaped HS-profile at low heteroplasmy levels (and high heteroplasmy levels as well). The upward undulation of the curve at low heteroplasmy levels, for example, does not necessarily imply a decrease in the negative selection intensity (which needs ***h'***, not HS, for correct evaluation). Also, this upward trend may be merely a result of the use of the 4th-order regression curve. The correct study of the selection at low heteroplasmy levels awaits more data and preferably ***h'***-based analysis.

P. Wonnapinij, P. F. Chinnery, D. C. Samuels, Previous estimates of mitochondrial DNA mutation level variance did not account for sampling error: Comparing the mtDNA genetic bottleneck in mice and humans. Am. J. Hum. Genet. 86, 540–550 (2010) .

Supplemental Figures

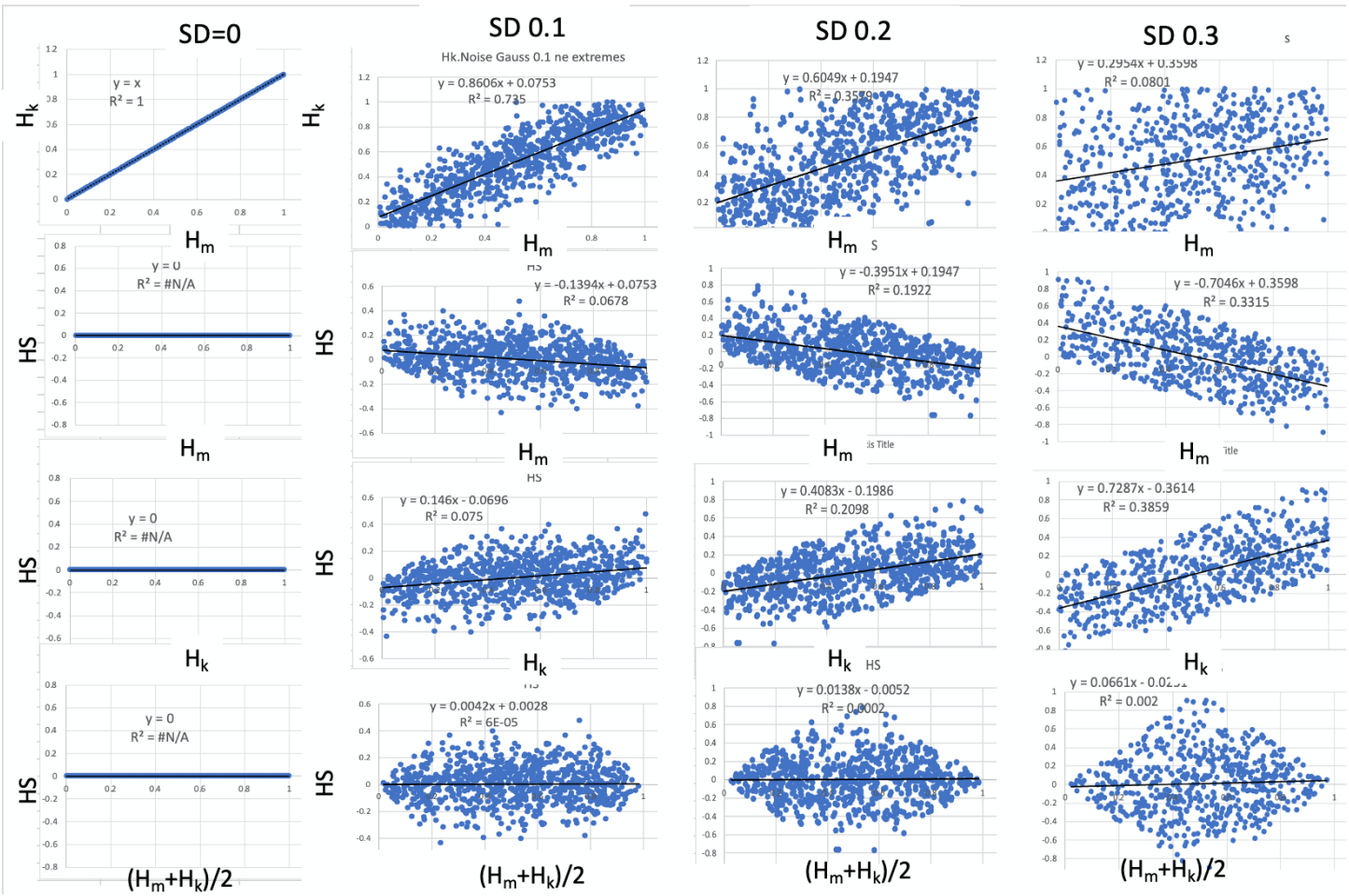

Figure S1. 'Regression analysis' of the simulated Mother-to-Child non-selective transmission data. Left column – the base 'perfect transmission' model: 'Child Heteroplasmy (H_k) equal to the Mother's heteroplasmy (H_m). Columns to the right show the effects of the progressive increase of the Gaussian variance added to both H_k and H_m (amounts of added variance are shown of the top: SD=0 to SD=0.3). Evidently, there is a marked decrease of the H_k vs. H_m correlation (top row), an increase of the (negative) slope of heteroplasmy shift (HS) vs. Mother's heteroplasmy (H_m) correlation (second row) and an increase of the (positive) slope of the HS vs. Child heteroplasmy (H_k) correlations (third row). Bottom row: RTM effect is nullified when the symmetrical variable, the average of mother's and child's heteroplasmy ($H_m + H_k$)/2 is used. See Methods for details of simulation.

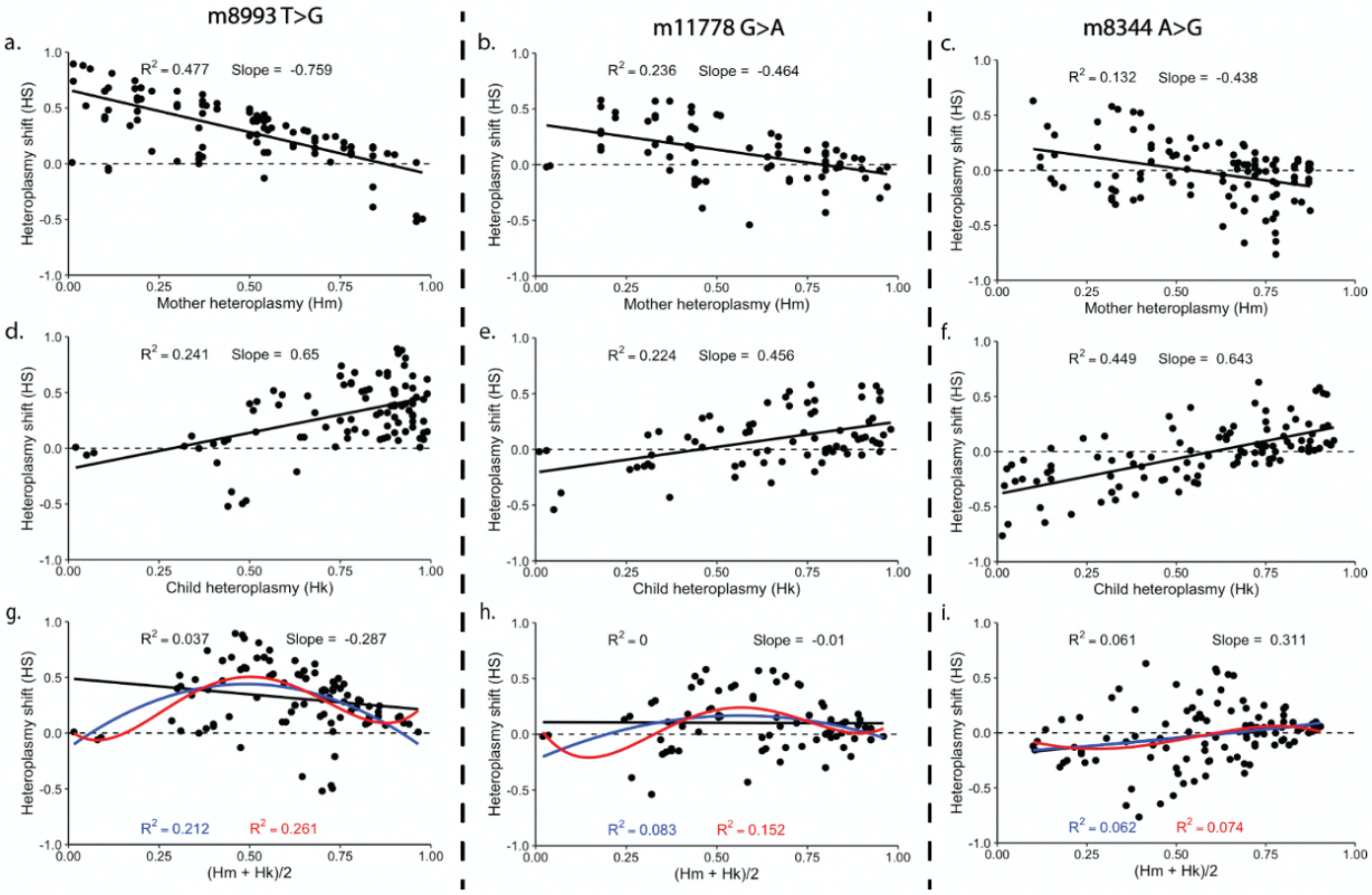

Figure S2. 'Regression analysis' of human mtDNA mutations 8993, 11778 and 8344 reveals the presence of RTM and underlying arch-shape (**g, h**), or not arch-shape (**i**) selection patterns. A negative correlation between HS and H_m (upper row) and a comparable positive correlation between HS and Hk (middle row) suggest the presence of RTM. In the third row, **g-i**, we use the average of mother and child heteroplasmies as an independent variable, which allows to cancel out the RTM effect and reveal the underlying selection patterns. We use non-linear regression to visualize the arch-shape patterns where present (blue, quadratic regression, and red, quartic regression). Note that m8344 A>G mutation does not show the arched-shaped profile typical for other 3 mutations discussed in this study, which reassures us that arched profile is not a universal artifact of the analysis, but a specific feature of some but not all mtDNA mutations.

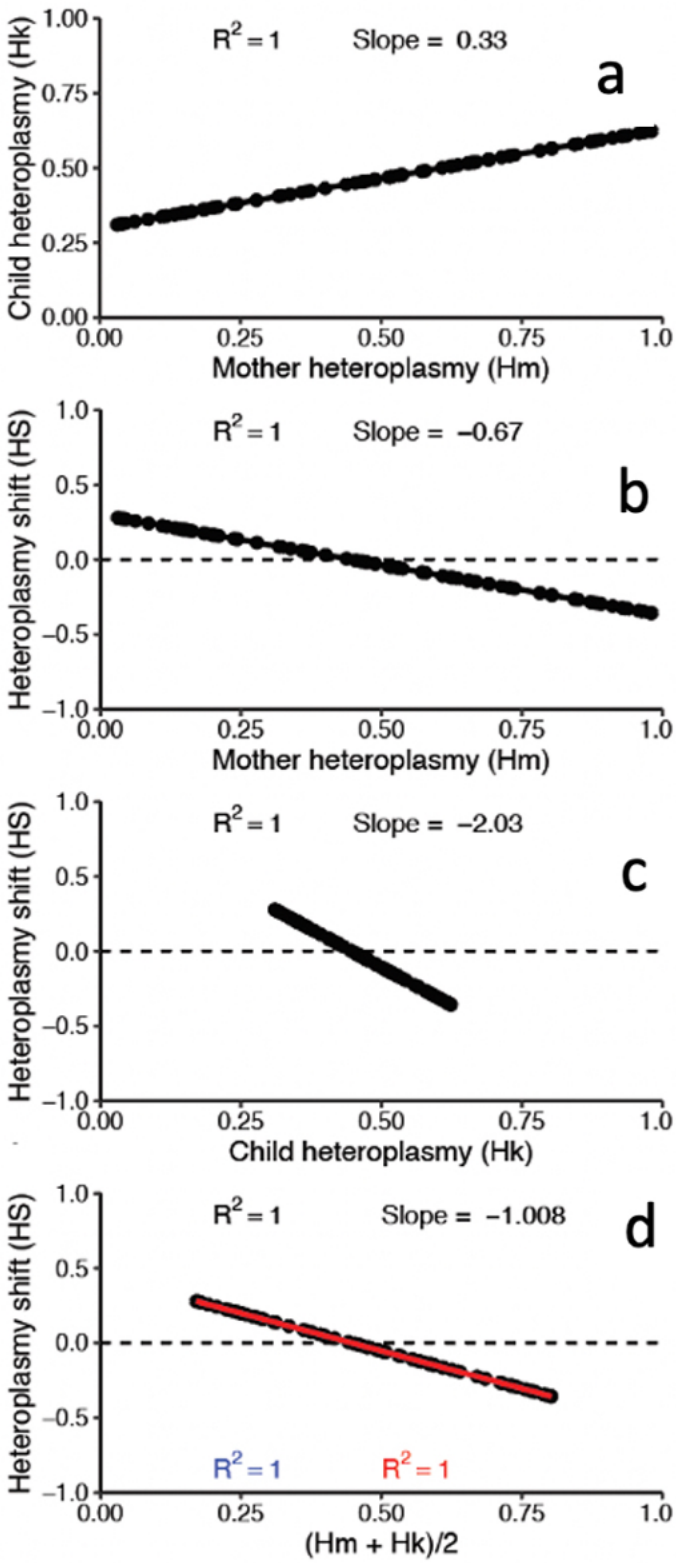

Figure S3. A linearly descending germline selection profile results in linearly descending correlation between heteroplasmy shift and heteroplasmy **both** in mothers **and** in children.

In this simulation we generated 75 { Hm,Hk} datapoints where Hm values were randomly distributed between 0 and 1, and Hk were generated using a linear function representing the descending germline selection profile. The function used wassimply the regression line of the experimental m3243A>G dataset (y=0.33x+0.3). This figure shows the regular 'RTM analysis' of the simulated data.

Importantly, the correlation between heteroplasmy c shift and child heteroplasmy (c) is negative, similarly to the orrelation between heteroplasmy shift and mother's heteroplasmy (b). This is in direct contradiction with the pattern observed in the experimental data (compare Fig. b and c).

Method: The simulated {H_m, H_K} dataset was generated using the linear function identical to that of the experimental m3243A>G dataset (**Fig. 2a**). As with the 'RTM-only' dataset in the previous section, we used 0.0001 steps to generate 10,000 data pairs. The resulting dataset was processed in the same way as the RTM-only dataset

The same conclusion can be obtained analytically – screenshot on the right to be transcribed.

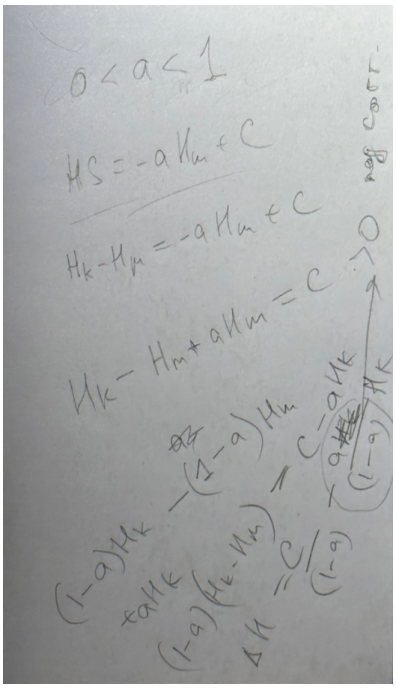

0<a<1

$HS = -aH_m + C$
$H_{ch} - H_m = -aH_m + C$
$H_{ch} - H_m + aH_m = C$

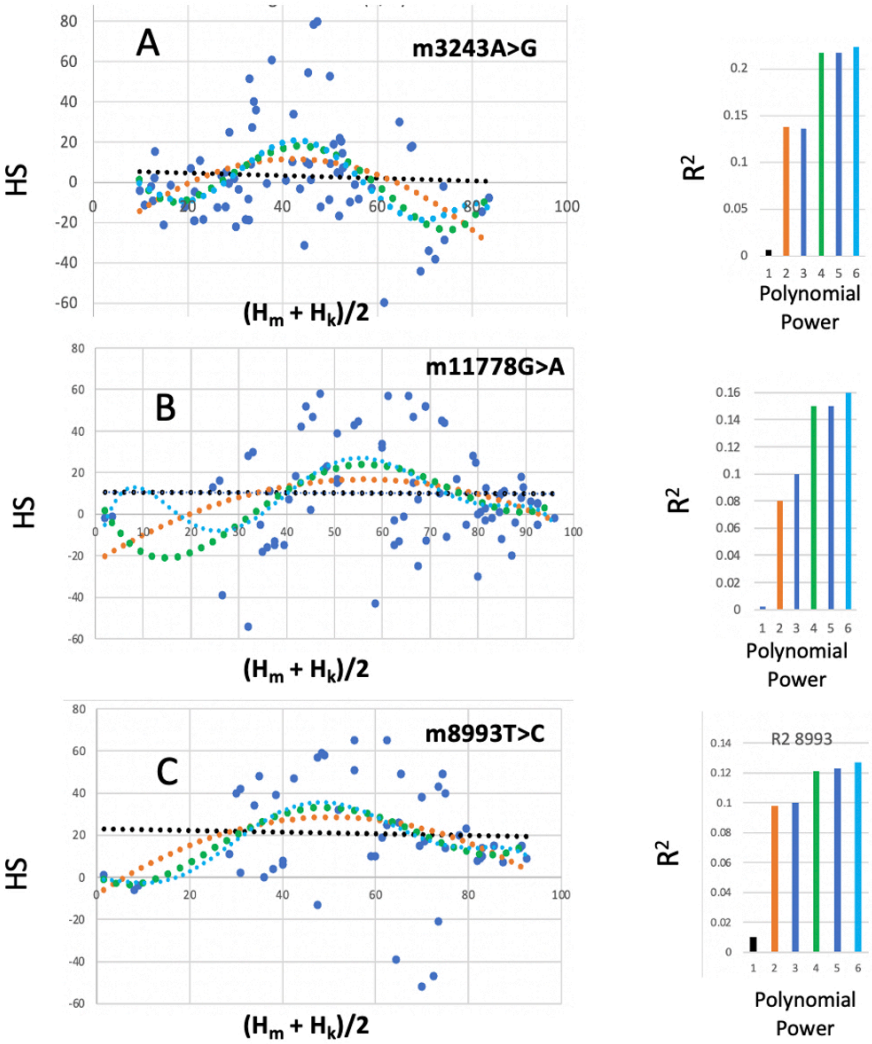

Figure S4 . Higher order regression analysis of the inheritance patterns of pathogenic mtDNA mutations reveals complex behavior around low heteroplasmy levels. As heteroplasmy decreases, an arch *consistently* (i.e., in all mutations that showed an arch in their germline selection profile) turns into a reverse arch, which converges to zero from the negative side. Whereas the data is insufficient for any statistically reliable conclusions, this observation is reassuring in that selection profile that is revealed in our studies, indeed, in accordance with biological expectations, converges to zero from the negative side. This behavior is more consistent with the hypothesis of negative selection at low heteroplasmy levels than mere arch described by a quadratic function. Selection is a proportional process (selection is changing existing heteroplasmy by a certain factor, rather by a certain absolute quantity). Therefore, as heteroplasmy approaches zero, HS is expected to converge to zero, not to diverge into the negative, as it necessarily does in the quadratic arch profile. The analysis presented in this figure, therefore, implies that the data are actually compatible with the negative selection scenario and that there is no contradiction between the arching profile and the expectation of convergence to zero. Of course, the above arguments are merely illustrative, and their goal is not to confirm any conclusions made in this study, but rather to show that the conclusions of this study are not contradictory.

Bar graphs on the right justify the use of 4th power regression: R^2 increases substantially when power is increased from 3^{d} to 4th, but there is no substantial additional gain in R^2 as we moved the 5th and 6th power. The curves' color corresponds to the color of the bars. The cueves of the 3d and 5th power (dark blue bars) are not shown.

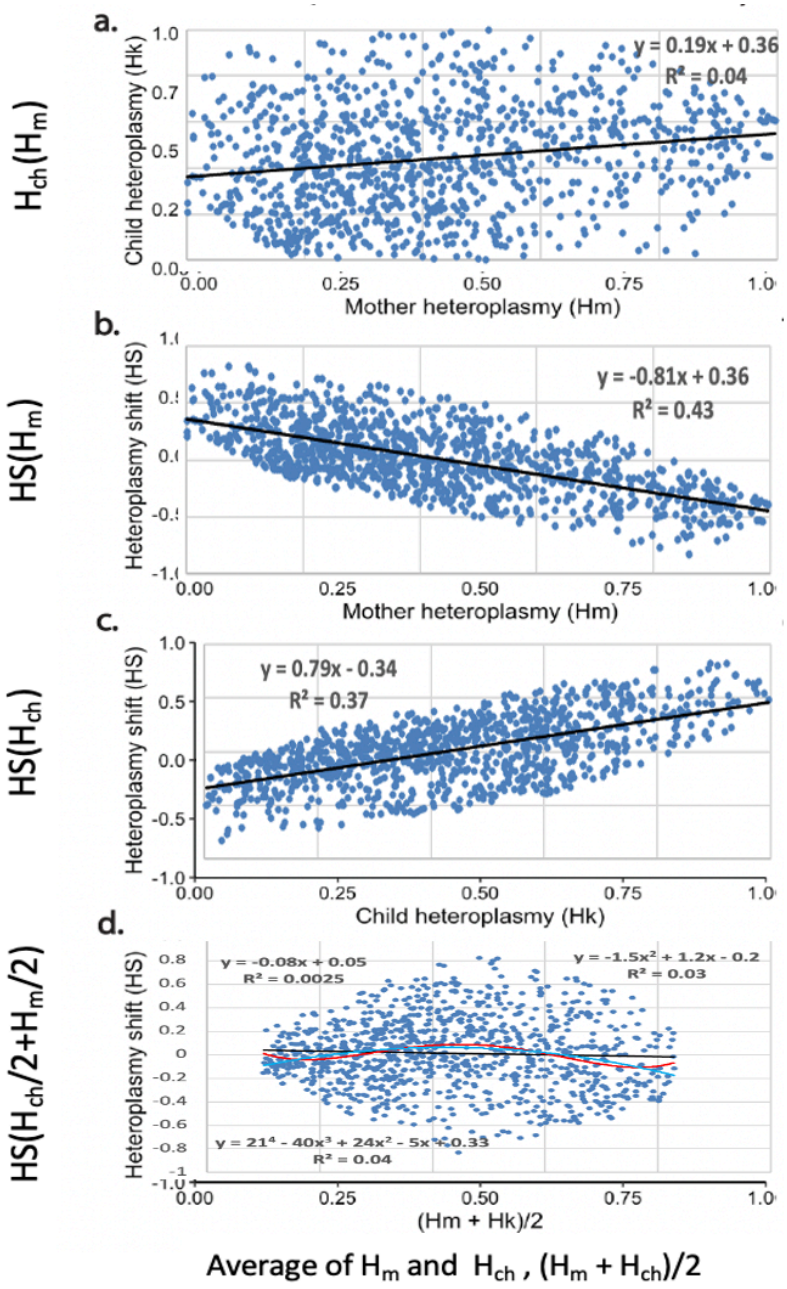

Figure S5. Pilot simulation using the model that combines germline selection and the RTM effect. See **Fig 2** caption for details.